Electromagnetic effects on toroidal momentum transport

M. Ansar Mahmood, A. Eriksson, and J. Weiland
Department of Radio and Space Science, Chalmers University of Technology, EURATOM/VR Association, SE-41296 Göteborg, Sweden

(Received 28 April 2010; accepted 13 October 2010; published online 16 December 2010)

A parametric study of electromagnetic effects on toroidal momentum transport has been performed. The work is based on a new version of the Weiland model where symmetry breaking toroidicity effects derived from the stress tensor have been taken into account. The model includes a self-consistent calculation of the toroidal momentum diffusivity, which contains both diagonal and off-diagonal contributions to the momentum flux. It is found that electromagnetic effects considerably increase the toroidal momentum pinch. They are sometimes strong enough to make the total toroidal momentum flux inward. [doi:10.1063/1.3511441]

I. INTRODUCTION

It is broadly believed that plasma rotation plays a crucial role in the suppression of turbulence and transport in fusion devices, therefore affecting their performance. In order to be able to confidently extrapolate our knowledge of plasma rotation to future fusion devices, toroidal momentum transport needs to be well understood. This is of particular importance for the prediction of ITER scenarios, where low levels of toroidal rotation are expected due to the large inertia and low torque compared to present devices. It is also important to understand the toroidal momentum transport in plasmas with internal transport barriers (ITB) in present devices since momentum transport generates rotational shear which is important for the formation of ITBs.[1]

The global confinement times and the diffusivities of energy and momentum have previously been assumed to be equal or predicted to be comparable.[2–4] Recent experimental studies[5,6] do, however, contradict these results and have yielded an effective Prandtl number (ratio of the effective momentum diffusivity ($\chi_{\phi,\mathrm{eff}}$) and an effective ion heat diffusivity ($\chi_{i,\mathrm{eff}}$)) substantially below 1. This discrepancy could be resolved as suggested by various studies through the existence of momentum pinch (inward flow of momentum flux), which is anticipated as the result of symmetry breaking effects on toroidal momentum transport.[7–18] The first effect of this type[8,9] was identified as the effect of an asymmetric eigenfunction on the average of the parallel mode number which is needed for the parallel momentum transport. This parallel momentum can, for practical purposes, be used as an approximation for the toroidal momentum. Recently, symmetry breaking effects of toroidicity were also found,[12–14,16] which are usually stronger than those caused by the flow shear on the eigenfunction.[7–11] A recent review on theoretical developments and experimental analysis of momentum transport and rotation can be found in Ref. 19.

Of various effects influencing the toroidal momentum transport, electromagnetic effects have been little studied. The present paper addresses these effects along with the detailed study of other parameters such as density and temperature gradients, electron to ion temperature ratio, magnetic shear, collisions, and plasma elongation. An interesting new aspect is that electromagnetic effects considerably increase the toroidal momentum pinch. Furthermore, they are sometimes strong enough to even get net (effective) momentum pinch, as compared with the corresponding electrostatic case.

The paper is organized as follows. In Sec. II a brief summary of the transport model we use is given. The results and discussions thereof are presented in Sec. III. Section IV contains our conclusions.

II. TOROIDAL MOMENTUM TRANSPORT MODEL

The transport model used here is an extended version of the Weiland model which includes a self-consistent treatment of the toroidal velocity,[10] taking symmetry breaking effects on toroidal momentum transport into account. The symmetry breaking effects are derived from the stress tensor.[16] The detailed derivations of different aspects of the model can be found elsewhere.[10,16,20–22] Here, a brief summary with focus on toroidal momentum transport is presented.

The model describes quasilinear transport due to ion temperature gradient (ITG) and trapped electron (TE) mode turbulence using fluid descriptions for the ion and trapped electron species. The particle, heat, and toroidal momentum fluxes ($\Gamma_n, \Gamma_T, \Gamma_\phi$) and their corresponding effective diffusivities (D, χ, χ_ϕ) are obtained from the time average of the ITG/TE mode perturbations in density (n), temperature (T), and toroidal velocity (v_ϕ) as $\Gamma_n = \mathrm{Re}\langle v_{E_r}^* \delta n\rangle = -D\nabla n$, $\Gamma_T = \mathrm{Re}\langle v_{E_r}^* \delta T\rangle = -\chi \nabla T$, and $\Gamma_\phi = m_i n\ \mathrm{Re}\langle v_{E_r}^* \delta v_\phi\rangle = -m_i n \chi_\phi \nabla v_\phi$, where v_{E_r} is the $\mathbf{E}\times\mathbf{B}$ drift velocity, $*$ means complex conjugate, and m_i is the mass of the main ions.

The toroidal velocity used to calculate the toroidal momentum flux is approximated as $v_\phi \approx v_\parallel - (B_\theta/B)v_\theta$, where θ refers to the poloidal direction. The perturbation in parallel ion velocity ($\delta v_{\parallel i}$) is calculated from the parallel momentum balance in the presence of a zero order background flow as

$$\delta v_{\parallel i} = -\frac{k_\theta D_B}{\omega - 2\omega_{Di}} \frac{dv_\parallel}{dr}\hat{\phi} + \frac{k_\parallel c_s^2 - v_\parallel \omega_{De}}{\omega - 2\omega_{Di}} f(\hat{\phi}, \hat{P}, \hat{A}_\parallel), \qquad (1)$$

where

$$f(\hat{\phi},\hat{P},\hat{A}_{\parallel}) = \hat{\phi} + \frac{1}{\tau}\hat{P} - \frac{\tilde{\omega} + (1+\eta_i)/(\epsilon_n\tau)}{\widetilde{k_{\parallel}c_s}}\hat{A}_{\parallel}. \tag{2}$$

Here, $\omega=\omega_r+i\gamma$ is the wave frequency, $\eta_i=L_n/L_{T_i}$ is the ratio of density to temperature length scales, $\epsilon_n=2L_n/R$, $\tau=T_e/T_i$ is the temperature ratio, $D_B=\rho_s c_s$, ρ_s is the gyroradius, c_s is the ion acoustic velocity, and k_θ, $k_\parallel$, and k_x are the wave numbers in the poloidal, parallel, and radial directions, respectively. Further, $\tilde{}$ denotes normalization by ω_{De} which is the electron drift frequency due to the magnetic field gradient and curvature, $\omega_{Dj}(j=e,i)=\mathbf{k}\cdot\mathbf{v}_{Dj}$ where $\mathbf{v}_{Dj}=T_j/(m_j\Omega_j)\hat{\mathbf{b}}\times(\nabla B/B+\hat{\mathbf{b}}\cdot\nabla\hat{\mathbf{b}})$, with Ω_j as the gyrofrequency and $\mathbf{B}=B\hat{\mathbf{b}}$. We also use $\hat{\phi}=e\phi/T_e$ and $\hat{A}_{\parallel}=eA_{\parallel}/T_e$ which are the normalized electrostatic and electromagnetic potentials, respectively. The normalized pressure perturbation, which is also a function of $\hat{\phi}$, is denoted by $\hat{P}=\delta P/P_0$. The electrostatic and electromagnetic potentials are related to each other through the electron continuity equation, the perturbed electron temperature, and Ampere's law as

$$A_{\parallel} = \frac{k_{\parallel}(\omega_{*e}-\omega)}{\omega(\omega_{*e}-\omega)+\omega_{De}[\omega-\omega_{*e}(1+\eta_e)]+k_{\perp}^2\rho_s^2k_{\parallel}^2v_A^2}\phi, \tag{3}$$

where $\omega_{*e}=k_\theta\rho_s c_s/L_n$ is the electron diamagnetic drift frequency, v_A is the Alfvén velocity, and $k_\perp$ is the perpendicular wave number given by $k_\perp^2=k_\theta^2(1+\hat{s}^2\theta^2)$. The effective magnetic shear $\hat{s}$ depends on the plasma elongation parameter κ (ratio between the vertical and horizontal plasma radii) and magnetic shear s as[23,24] $\hat{s}=\sqrt{2s-1+\kappa^2(s-1)^2}$. The magnetic shear s is defined as $(r/q)dq/dr$, where q is the magnetic safety factor.

The first term in Eq. (1) is the $\mathbf{E}\times\mathbf{B}$ convection of the background velocity and gives diagonal toroidal momentum flux, whereas the second term gives off-diagonal pinch terms proportional to a combination of $\langle k_\parallel\rangle$ and ω_D. The stress tensor toroidal/curvature effects[16] appearing through ω_D are extended features of the current Weiland model, which were absent in its previous version.[10,11] As it appears, these effects increase the outward flux as well as the momentum pinch.[16] Neglecting the poloidal flow terms, the diagonal toroidal momentum flux is derived from quasilinear theory with $v_{E_r}=-ik_\theta D_B\hat{\phi}$ and

$$\delta v_\phi = -\frac{k_\theta D_B}{\omega-2\omega_{Di}}\frac{dv_\phi}{dr}\hat{\phi}. \tag{4}$$

Assuming that $\mathbf{E}\times\mathbf{B}$ convection is the main nonlinear saturation mechanism, the potential fluctuation is given by $\hat{\phi}=\gamma/(k_x\rho_s k_\theta c_s)$.[20,21] The total toroidal momentum flux is thus approximated as

$$\Gamma_\phi \approx -m_i n\frac{\gamma^3/k_x^2}{(\omega_r-2\omega_{Di})^2+\gamma^2}\frac{dv_\phi}{dr} + \Gamma_{\phi\mathrm{OD}}, \tag{5}$$

where the first term is the diagonal diffusion and the second term $\Gamma_{\phi\mathrm{OD}}$ contains the off-diagonal pinch terms given as

$$\Gamma_{\phi\mathrm{OD}} = m_i n k_\theta D_B(c_s^2\langle k_\parallel\rangle - \omega_{De}v_\phi)\mathrm{Re}\left\langle \frac{i\hat{\phi}^*}{\omega-2\omega_{Di}}f(\hat{\phi},\hat{P},\hat{A}_{\parallel})\right\rangle. \tag{6}$$

The perpendicular Reynolds stress contribution,[10] which is very small compared to the parallel contribution, is neglected in approximating the total toroidal momentum flux [Eqs. (5) and (6)]. This is, however, retained in the numerical results. We write the total or effective momentum diffusivity as $\chi_{\phi,\mathrm{eff}}=\chi_{\phi,D}+\chi_{\phi,\mathrm{OD}}$, where $\chi_{\phi,D}$ is the diagonal diffusivity

$$\chi_{\phi,D} = \frac{\gamma^3/k_x^2}{(\omega_r-2\omega_{Di})^2+\gamma^2} \tag{7}$$

and $\chi_{\phi,\mathrm{OD}}$ is the off-diagonal contribution from the Reynolds stress, parallel velocity,[10] and symmetry breaking effects of curvature[16]

$$\chi_{\phi,\mathrm{OD}} = -\left(\frac{\epsilon}{q}\right)\frac{k_r k_\theta D_B^2}{dv_\phi/dr}\mathrm{Re}\left\langle\hat{\phi}^*\left(\hat{\phi}+\frac{1}{\tau}\hat{P}\right)\right\rangle - \frac{k_\theta D_B}{dv_\phi/dr}(c_s^2\langle k_\parallel\rangle - \omega_{De}v_\phi)\mathrm{Re}\left\langle\frac{i\hat{\phi}^*}{\omega-2\omega_{Di}}f(\hat{\phi},\hat{P},\hat{A}_{\parallel})\right\rangle. \tag{8}$$

The diagonal term, which is usually the dominant term for toroidal momentum transport in the present model, seems first to have been obtained for the parallel motion using gyrofluid equations in Ref. 25. For momentum transport, this was also obtained from gyrofluid equations in Refs. 12 and 13, while a fluid derivation from the stress tensor was made in Ref. 14. The off-diagonal contribution to the momentum diffusivity was also first obtained from gyrofluid equations in Refs. 12 and 13. In Ref. 13, gyrokinetic results, consistently computed with a gyrokinetic code, were also reported.

For standard drift waves with up-down symmetric eigenfunctions, $\langle k_\parallel\rangle$, which is the flux surface average of $k_\parallel$, is zero. Radial flow shear $(dv_\phi/dr, dv_\theta/dr)$ can produce a mode shift which leads to a finite value of $\langle k_\parallel\rangle$ and this may lead to an inward flow of toroidal momentum.[7–9] The toroidicity, on the other hand, enhances the pinch due to symmetry breaking effects and also due to the resonant denominator.

The average parallel mode number $\langle k_\parallel\rangle$ is calculated from the eigenfunction, which is consistently computed by applying the first step of the direct method (i.e., the radial eigenvalue problem) by Taylor and Wilson[26] as shown in Ref. 16. Thus, both flow shear and toroidal effects give symmetry breaking for the parallel wave number. We note that electromagnetic effects are another nonadiabatic effect that increases the toroidal momentum pinch in a similar way as found by Peeters *et al.*[17] for electron trapping. In Ref. 17, the mode structure along the field line was self-consistently computed using gyrokinetic approach in full toroidal geometry.

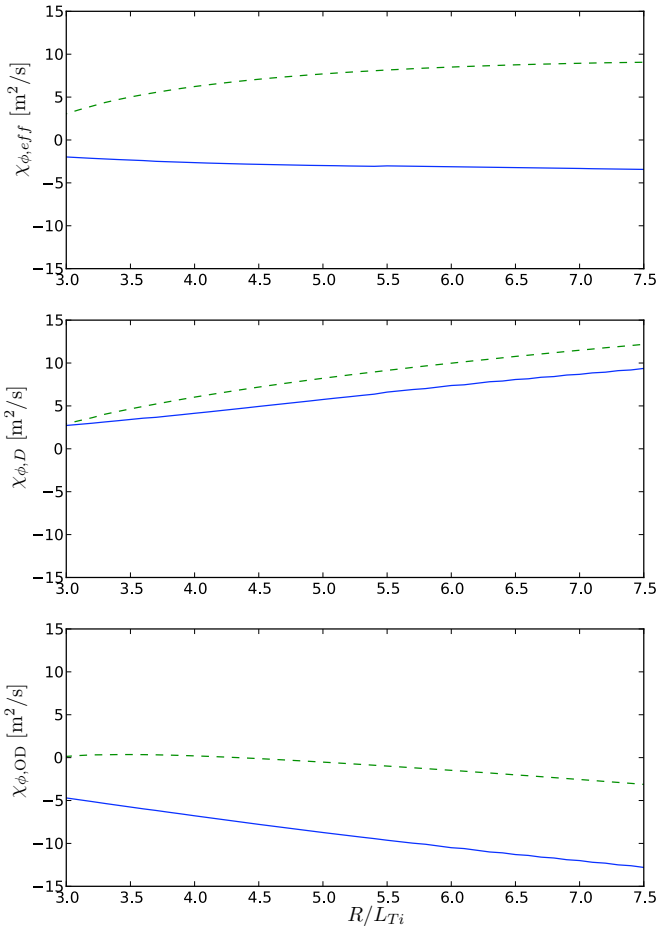

FIG. 1. (Color online) Effective momentum diffusivity $\chi_{\phi,\text{eff}}$ along with diagonal contribution $\chi_{\phi,D}$ and off-diagonal contribution $\chi_{\phi,\text{OD}}$ as a function of normalized ion temperature scale length R/L_{Ti} for the electromagnetic (solid) and electrostatic (dashed) cases. Other parameters are given in the beginning of Sec. III.

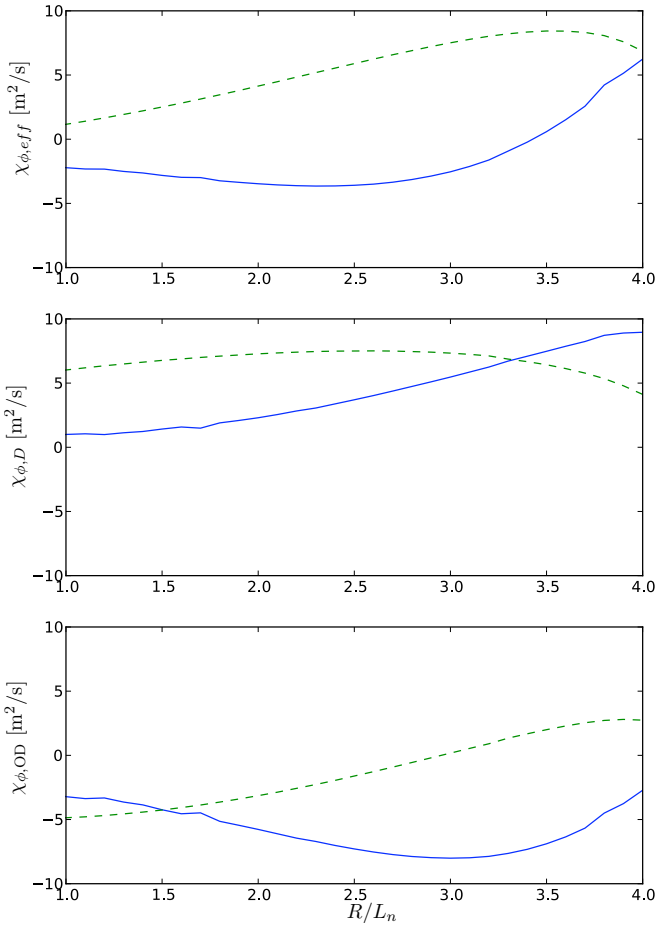

FIG. 2. (Color online) Effective momentum diffusivity $\chi_{\phi,\text{eff}}$ along with diagonal contribution $\chi_{\phi,D}$ and off-diagonal contribution $\chi_{\phi,\text{OD}}$ as a function of normalized density scale length R/L_n for the electromagnetic (solid) and electrostatic (dashed) cases. Other parameters are given in the beginning of Sec. III.

Neglecting the pinch contributions, the Prandtl number $\text{Pr}=\chi_{\phi,D}/\chi_{i,D}$ in the present version of the Weiland model is expressed as

$$\text{Pr} = \frac{(\omega_r - 5/3\omega_{Di})^2 + \gamma^2}{(\omega_r - 2\omega_{Di})^2 + \gamma^2}. \tag{9}$$

It is to be remarked here that the diagonal elements used to define the diagonal Prandtl number [Eq. (9)] are those that come out naturally from the derivation. They are also positive definite so they work well as diagonal elements from a numerical point of view. However, they depend on the eigenfrequency and through that on all gradients in the system. Thus they are not diagonal elements in a strict sense and this should be remembered in comparisons with experiment.

The Prandtl number defined in Eq. (9) is usually close to 1. However, close to marginal stability, e.g., near the axis in tokamaks, the real eigenfrequencies approach $5/3\omega_{Di}$ and the Prandtl number according to Eq. (9) is expected to be substantially below 1. The inclusion of pinch contributions, along with electromagnetic effects, further modifies the Prandtl number as will be discussed in Sec. III.

III. RESULTS AND DISCUSSIONS

The following dimensionless parameters are used in the present study: $q=3.1$, $s=0.6$, $R/L_{Ti}=4.6$, $R/L_{Te}=4.0$, $R/L_n=2.8$, $\tau=1$, $k_\theta\rho_s=0.23$, $f_t=0.5$ (f_t is the fraction of trapped electrons), $\kappa=1.25$, and the ratio of plasma and magnetic pressure for electrons $\beta_e=0.4\%$ (the electron density and temperature are $n_e=2.8\times10^{19}$ m^{-3} and $T_e=2.4$ keV). In the presented scans, one of these parameters is varied while keeping the others fixed.

Figure 1 displays the effective momentum diffusivity $\chi_{\phi,\text{eff}}$ as a function of the normalized ion temperature scale length R/L_{Ti} for the electromagnetic (solid) and electrostatic (dashed) cases. The diagonal and off-diagonal contributions, $\chi_{\phi,D}$ and $\chi_{\phi,\text{OD}}$, are also shown separately. It is evident that there is an effective momentum pinch when electromagnetic effects are taken into account. There is a small pinch contribution in the electrostatic case as well, but here the diagonal element dominates and so the net result is outward diffusion. The pinch is found to be increasing with increase in R/L_{Ti}.

A scaling with the normalized density scale length R/L_n is displayed in Fig. 2. The trend is similar to the scaling with the temperature scale length: electromagnetic effects introduce a net effective momentum pinch which increases

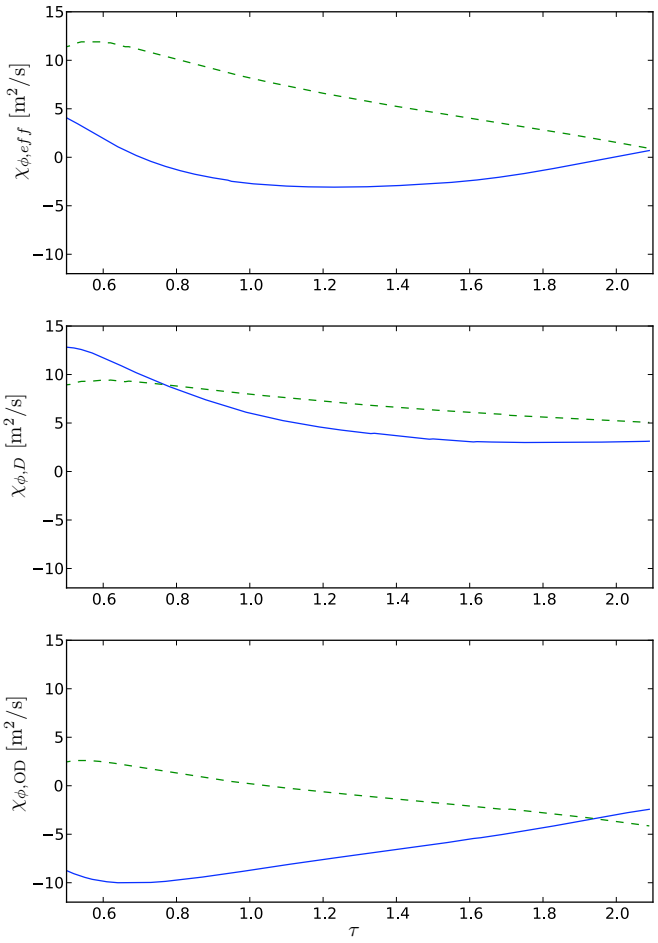

FIG. 3. (Color online) Effective momentum diffusivity $\chi_{\phi,\text{eff}}$ along with diagonal contribution $\chi_{\phi,D}$ and off-diagonal contribution $\chi_{\phi,\text{OD}}$ as a function of electron to ion temperature ratio τ for the electromagnetic (solid) and electrostatic (dashed) cases. Other parameters are given in the beginning of Sec. III.

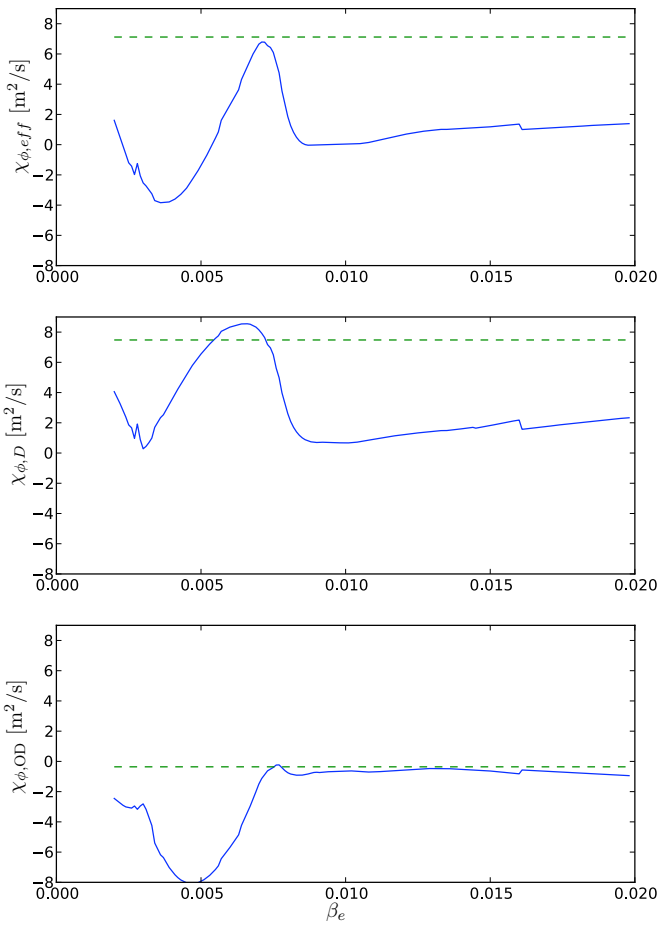

FIG. 4. (Color online) Effective momentum diffusivity $\chi_{\phi,\text{eff}}$ along with diagonal contribution $\chi_{\phi,D}$ and off-diagonal contribution $\chi_{\phi,\text{OD}}$ as a function of the ratio of plasma and magnetic pressure for electrons β_e for the electromagnetic (solid) and electrostatic (dashed) cases. Other parameters are given in the beginning of Sec. III.

with increasing R/L_n. However, this trend is broken at a certain R/L_n. This is because for very large R/L_n values, η_i $(=L_n/L_{Ti})$ also decreases, which results in a decrease in the growth rate of the dominated ITG mode and hence a decrease in the momentum flux.

Figure 3 shows a scan with electron to ion temperature ratio τ. We note that the effective momentum diffusivity $\chi_{\phi,\text{eff}}$ in the electrostatic case is positive for small values of τ and appears to be negative for large values of τ. This is because the diagonal momentum diffusivity $\chi_{\phi,D}$ decreases, while the off-diagonal contribution $\chi_{\phi,\text{OD}}$ gives pinch with increasing τ. The net effect is thus an electrostatic momentum pinch for large τ values. When electromagnetic effects are taken into account, the effective momentum diffusivity $\chi_{\phi,\text{eff}}$ is negative (pinch) for small values of τ and positive for large values, i.e., for $\tau>2$. In this case, we can see the dominant electromagnetic pinch contribution $\chi_{\phi,\text{OD}}$ to the total effective momentum diffusivity. The maximum effective pinch is found to occur at $\tau=1.23$.

A scan with β_e is presented in Fig. 4. We find strong electromagnetic effects and an effective momentum pinch in the range $0.23\%<\beta_e<0.55\%$, with maximum pinch occurring at $\beta_e\approx 0.4\%$. As observed, the off-diagonal contribution $\chi_{\phi,\text{OD}}$ dominates in this range. Further increase in β_e (i.e., for $\beta_e>0.55\%$) introduces a region of net outward momentum diffusion with maximum at $\beta_e\approx 0.7\%$; this is also the value at which minimum electromagnetic effects are noted. Here, dominance of the diagonal element $\chi_{\phi,D}$ is evident. The nonmonotonic dependence of the momentum diffusivity found in Fig. 4, particularly that of the diagonal element $\chi_{\phi,D}$, which appears to be inconsistent with the result found in Ref. 14, can be understood by examining the magnetohydrodynamic (MHD) β limit for the parameters used here. The MHD β limit would typically be around $\alpha=0.5$, where α is the MHD parameter given by

$$\alpha = 2q^2\beta_e\left[1+\eta_e+\frac{1}{\tau}(1+\eta_e)\right]. \tag{10}$$

For the parameters used here with rather large q, we get a relatively small β limit, i.e., $\alpha=0.43$ at $\beta_e=0.3\%$, which is roughly where the growth of the diagonal element starts. The growth of the diagonal element is thus due to increased growth rate. The reduction of the beta limit from 0.5 to 0.43 is well within the expectations due to the kinetic ballooning mode.[27] We can then conclude that the region with strong

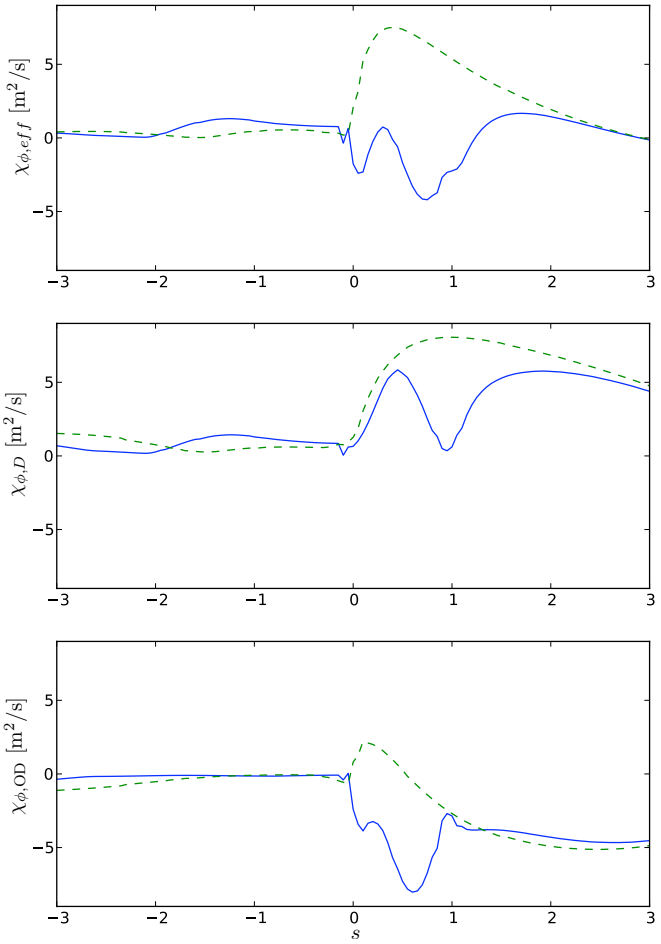

FIG. 5. (Color online) Effective momentum diffusivity $\chi_{\phi,\text{eff}}$ along with diagonal contribution $\chi_{\phi,D}$ and off-diagonal contribution $\chi_{\phi,\text{OD}}$ as a function of magnetic shear s for the electromagnetic (solid) and electrostatic (dashed) cases. Other parameters are given in the beginning of Sec. III.

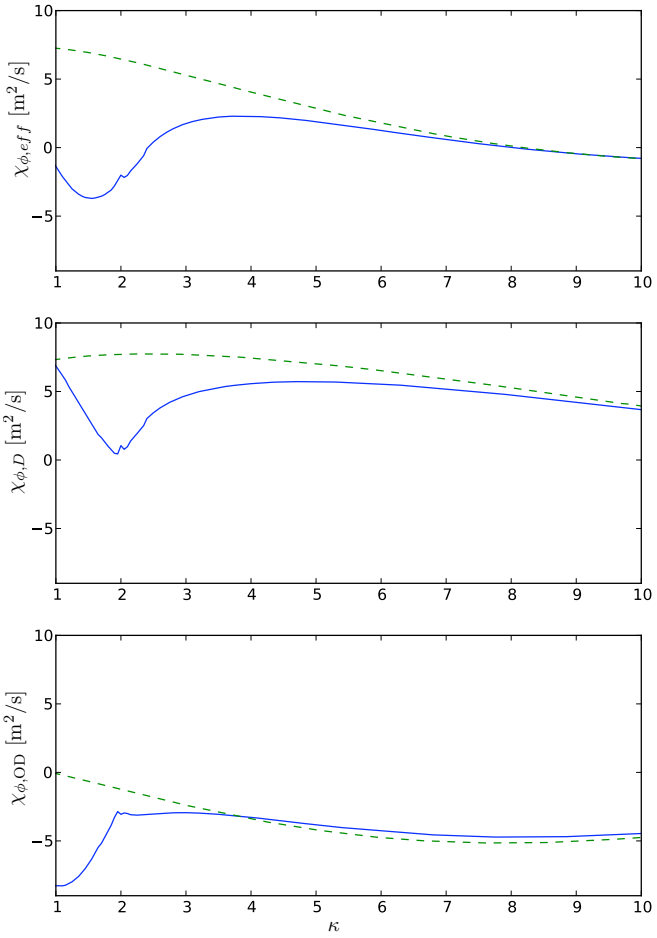

FIG. 6. (Color online) Effective momentum diffusivity $\chi_{\phi,\text{eff}}$ along with diagonal contribution $\chi_{\phi,D}$ and off-diagonal contribution $\chi_{\phi,\text{OD}}$ as a function of plasma elongation κ for the electromagnetic (solid) and electrostatic (dashed) cases. Other parameters are given in the beginning of Sec. III.

momentum pinch will correspond to typical experimental situations. For large β values, we find zero or very small diffusion, which corresponds to the second stability regime of electromagnetic ballooning modes.

The effect of magnetic shear s is illustrated in Fig. 5. For small values of positive magnetic shear, there is a large net (effective) outward diffusion in the electrostatic case and a net (effective) pinch in the electromagnetic case. We also note that large positive magnetic shear tends to reduce the electromagnetic effects on momentum diffusivity. This may be due to the reason that increasing magnetic shear increases the perpendicular wave number, which leads to the reduction of electromagnetic effects [Eq. (3)]. Large positive magnetic shear also reduces the momentum transport by stabilizing the linear eigenmodes. The net momentum diffusivity for negative magnetic shear is found to be very small in electrostatic case as well as in electromagnetic case. From Fig. 5, we observe some irregular dependence on magnetic shear. This is because in the transport model used here, magnetic shear has two effects. It introduces convective damping, which is stabilizing, and then makes the mode profile more localized, which is destabilizing. Thus one effect may dominate in some regime and the other in another regime. Furthermore, our particular model gives zero transport for zero shear but that differences between different models are restricted to a region close to zero shear.

Figure 6 shows a scaling with the plasma elongation parameter κ. Strong electromagnetic effects are evident in the scan, introducing a large net momentum pinch between $\kappa=1$ and $\kappa=2$. The electromagnetic effects on momentum diffusivity vanish for large values of κ. This is expected as increasing κ increases the effective magnetic shear, which then leads to the reduction of electromagnetic effects. The scan is extended to very large values of κ (which are not practical) only to see the limit where electromagnetic effects diminish. The limit is found to be considerably larger than normally expected and this is due to the magnetic shear value for the present scan $s=0.58$, which, as shown in Fig. 5, gives strong electromagnetic effects. We also observe that the electromagnetic effects are reduced for considerably smaller values of κ in the off-diagonal contribution $\chi_{\phi,\text{OD}}$ than in the diagonal one $\chi_{\phi,D}$.

A scaling with the fraction of trapped electrons f_t is shown in Fig. 7. We note that in the electrostatic case, the diagonal momentum diffusivity $\chi_{\phi,D}$ increases, as expected, while the off-diagonal contribution $\chi_{\phi,\text{OD}}$ decreases (and even introduces a pinch) with increasing f_t. The net effect is, however, an outward momentum diffusion which appears to

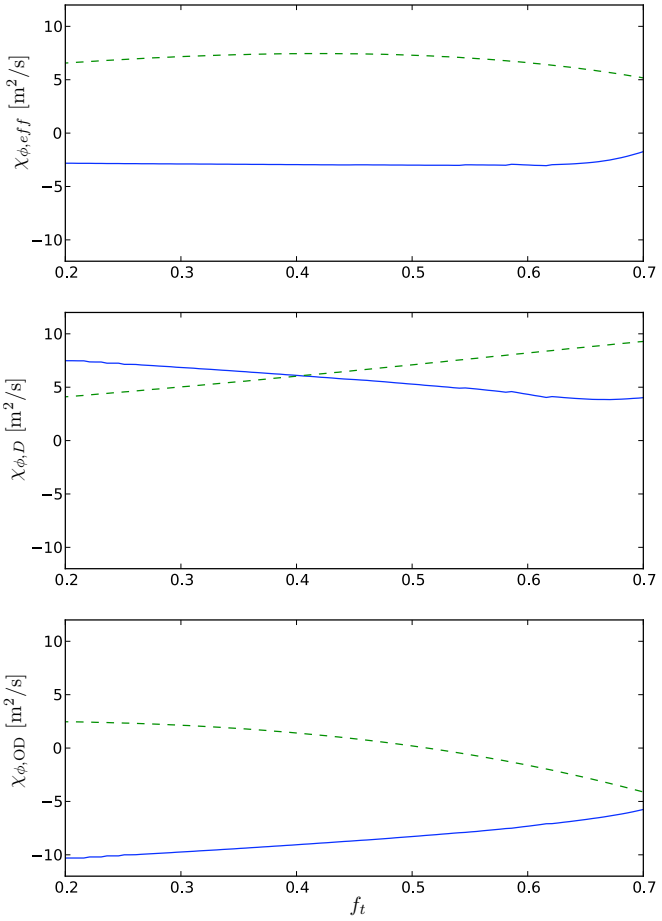

FIG. 7. (Color online) Effective momentum diffusivity $\chi_{\phi,\mathrm{eff}}$ along with diagonal contribution $\chi_{\phi,D}$ and off-diagonal contribution $\chi_{\phi,\mathrm{OD}}$ as a function of the fraction of trapped electrons f_t for the electromagnetic (solid) and electrostatic (dashed) cases. Other parameters are given in the beginning of Sec. III.

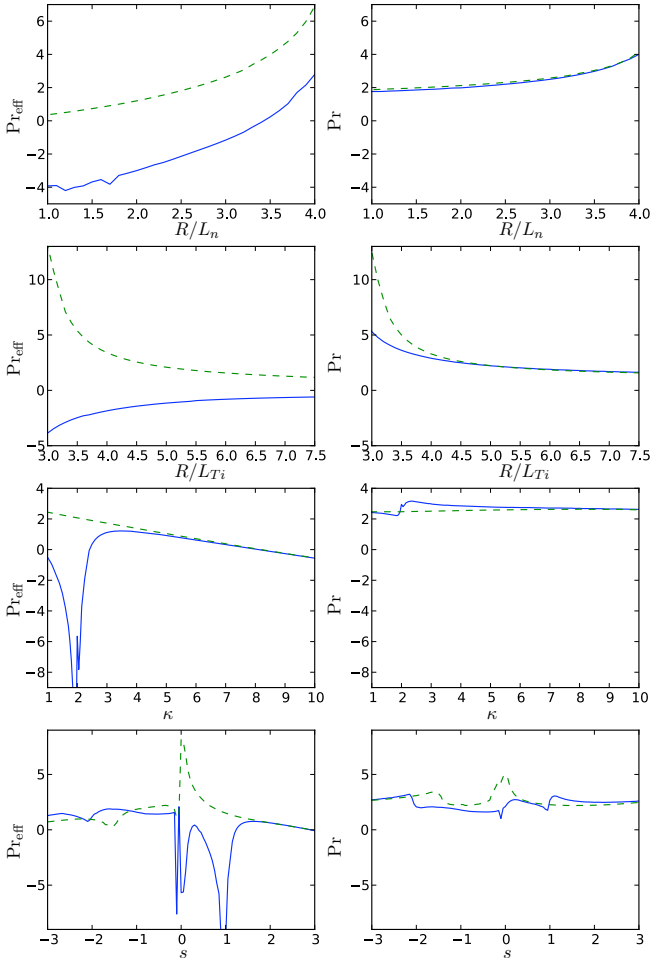

FIG. 8. (Color online) Effective Prandtl number $\mathrm{Pr}_{\mathrm{eff}}=\chi_{\phi,\mathrm{eff}}/\chi_{i,\mathrm{eff}}$ (left) and Prandtl number $\mathrm{Pr}=\chi_{\phi,D}/\chi_{i,D}$ (right) vs R/L_n, R/L_{Ti}, τ, κ, and s. The solid curves represent the electromagnetic case and the dashed curves the electrostatic case.

be weakly affected by f_t. A weak effect of f_t on the effective momentum diffusivity $\chi_{\phi,\mathrm{eff}}$ can also be seen in the electromagnetic case where net (effective) momentum pinch is found.

The role of collisions is found to be small for electrostatic momentum diffusivity. This is similar to the results found in Refs. 17 and 18. However, with the inclusion of electromagnetic effects, the effective momentum diffusivity is found to be very sensitive to collisions. A net outward diffusion is found in the absence of collisions while a net momentum pinch appears when collisions are taken into account for the selected parameters.

Figure 8 presents the scaling of the Prandtl number $\mathrm{Pr}=\chi_{\phi,D}/\chi_{i,D}$ (i.e., neglecting the off-diagonal contributions) and the effective Prandtl number $\mathrm{Pr}_{\mathrm{eff}}=\chi_{\phi,\mathrm{eff}}/\chi_{i,\mathrm{eff}}$ (i.e., retaining also the off-diagonal contributions) with different parameters of interest for the electromagnetic (solid) and electrostatic (dashed) cases. As observed, the inclusion of electromagnetic effects does not have any notable influence on the scaling of the Prandtl number Pr. However, strong electromagnetic effects are evident in the scaling of the effective Prandtl number $\mathrm{Pr}_{\mathrm{eff}}$. Here, the negative effective Prandtl numbers are due to the net momentum pinch caused by the inclusion of electromagnetic effects. We also note that the scaling of $\mathrm{Pr}_{\mathrm{eff}}$ with all the scanned parameters is stronger than that of Pr.

The trend of scaling with R/L_n is that a more peaked density profile results in a larger Prandtl (and effective Prandtl) number in the electrostatic case, whereas in the electromagnetic case, a flatter density profile gives a larger negative effective Prandtl number. For large temperature gradients, due to larger growth rates compared to the real eigenfrequencies, the Prandtl number Pr approaches unity as is expected according to Eq. (9). Furthermore, the effective Prandtl number $\mathrm{Pr}_{\mathrm{eff}}$ is slightly smaller than Pr due to the off-diagonal contributions and has a negative value with the inclusion of electromagnetic effects. When we move from large temperature gradients toward the threshold (in R/L_{Ti}), Pr and $\mathrm{Pr}_{\mathrm{eff}}$ increases. This trend is quite similar to what was found earlier from gyrokinetic calculations.[14]

It can also be seen in Fig. 8 that $\mathrm{Pr}_{\mathrm{eff}}$ in the electromagnetic case is large and negative in regions where plasma elongation and positive magnetic shear is small. This is consistent with the analysis of Figs. 5 and 6. For certain values of plasma elongation and magnetic shear, we find some singularities in the effective Prandtl number $\mathrm{Pr}_{\mathrm{eff}}$ because the

effective ion heat diffusivity $\chi_{i,\mathrm{eff}}$ vanishes for these values. This can happen because the off-diagonal elements $(\chi_{i,\mathrm{OD}})$ cancel the diagonal ones $(\chi_{i,D})$.

IV. CONCLUSIONS

It is shown in this paper that electromagnetic effects can significantly modify the properties of toroidal momentum transport in tokamak plasmas. Electromagnetic effects considerably increase the toroidal momentum pinch. They are sometimes strong enough to even get net (effective) momentum pinch, as compared with the corresponding electrostatic case. The strength of these effects and that of the momentum pinch depend strongly on local plasma parameters. A strong net momentum pinch has been found for large ion temperature gradient, approximately equal values of electron and ion temperatures, small positive magnetic shear, and for values of the plasma elongation parameter κ between 1 and 2. In these parametric regions, electromagnetic effects on toroidal momentum transport are strong and the effective Prandtl number $\mathrm{Pr}_{\mathrm{eff}}=\chi_{\phi,\mathrm{eff}}/\chi_{i,\mathrm{eff}}$ has large and negative values. However, for these optimum parameters, omitting collisions in the transport model gives a net outward momentum diffusion. Large negative values of the effective Prandtl number have also been found for small density gradients. Electromagnetic effects are reduced by increasing magnetic shear and plasma elongation.

ACKNOWLEDGMENTS

The authors would like to thank the anonymous referee for valuable suggestions which improved the paper. Discussions with Dr. Hans Nordman are gratefully acknowledged.

[1] V. V. Parail, Plasma Phys. Controlled Fusion **44**, A63 (2002).
[2] N. Mattor and P. H. Diamond, Phys. Fluids **31**, 1180 (1988).
[3] K.-D. Zastrow, W. G. F. Core, L.-G. Eriksson, M. G. Von Hellermann, A. C. Howman, and R. W. T. Künig, Nucl. Fusion **38**, 257 (1998).
[4] J. S. deGrassie, D. R. Baker, K. H. Burrell, P. Gohil, C. M. Greenfield, R. J. Groebner, and D. M. Thomas, Nucl. Fusion **43**, 142 (2003).
[5] D. Nishijima, A. Kallenbach, S. Günter, M. Kaufmann, K. Lackner, C. F. Maggi, A. G. Peeters, G. V. Pereverzev, B. Zaniol, and ASDEX Upgrade Team, Plasma Phys. Controlled Fusion **47**, 89 (2005).
[6] P. C. de Vries, K. M. Rantamäki, C. Giroud, E. Asp, G. Corrigan, A. Eriksson, M. De Greef, I. Jenkins, H. C. M. Knoops, P. Mantica, H. Nordman, P. Strand, T. Tala, J. Weiland, K.-D. Zastrow, and JET EFDA Contributors, Plasma Phys. Controlled Fusion **48**, 1693 (2006).
[7] R. R. Dominguez and G. M. Staebler, Phys. Fluids B **5**, 3876 (1993).
[8] X. Garbet, Y. Sarazin, and P. Ghendrih, Phys. Plasmas **9**, 3893 (2002).
[9] A. G. Peeters and C. Angioni, Phys. Plasmas **12**, 072515 (2005).
[10] J. Weiland and H. Nordman, *Proceedings of the 33rd EPS Conference on Plasma Physics* (European Physical Society, Rome, 2006), Vol. 30I, p. P-2.186.
[11] A. Eriksson, H. Nordman, P. Strand, J. Weiland, T. Tala, E. Asp, G. Corrigan, C. Giroud, M. De Greef, I. Jenkins, H. C. M. Knoops, P. Mantica, K. M. Rantamäki, P. C. de Vries, K.-D. Zastrow, and JET EFDA Contributors, Plasma Phys. Controlled Fusion **49**, 1931 (2007).
[12] T. S. Hahm, P. H. Diamond, O. D. Gurcan, and G. Rewoldt, Phys. Plasmas **14**, 072302 (2007).
[13] A. G. Peeters, C. Angioni, and D. Strintzi, Phys. Rev. Lett. **98**, 265003 (2007).
[14] D. Strintzi, A. G. Peeters, and J. Weiland, Phys. Plasmas **15**, 044502 (2008).
[15] I. Holod and Z. Lin, Phys. Plasmas **15**, 092302 (2008).
[16] J. Weiland, R. Singh, H. Nordman, P. Kaw, A. G. Peeters, and D. Strinzi, Nucl. Fusion **49**, 065033 (2009).
[17] A. G. Peeters, C. Angioni, Y. Camenen, F. J. Casson, W. A. Hornsby, A. P. Snodin, and D. Strintzi, Phys. Plasmas **16**, 062311 (2009).
[18] N. Kluy, C. Angioni, Y. Camenen, and A. G. Peeters, Phys. Plasmas **16**, 122302 (2009).
[19] J. S. deGrassie, Plasma Phys. Controlled Fusion **51**, 124047 (2009).
[20] J. Weiland and H. Nordman, in *Theory of Fusion Plasmas*, edited by J. Vaclavic, F. Troyon, and E. Sindoni (Editrice Compositori, Varenna, 1988), p. 451.
[21] H. Nordman and J. Weiland, Nucl. Fusion **29**, 251 (1989).
[22] J. Weiland, *Collective Modes in Inhomogeneous Plasma* (IOP, Bristol, 2000).
[23] D. D. Hua, X. Q. Xu, and T. K. Fowler, Phys. Fluids B **4**, 3216 (1992).
[24] F. D. Halpern, A. Eriksson, G. Bateman, A. H. Kritz, A. Pankin, C. M. Wolfe, and J. Weiland, Phys. Plasmas **15**, 012304 (2008).
[25] R. E. Waltz, R. R. Dominguez, and G. W. Hammett, Phys. Fluids B **4**, 3138 (1992).
[26] J. B. Taylor and H. R. Wilson, Plasma Phys. Controlled Fusion **38**, 1999 (1996).
[27] P. Andersson and J. Weiland, Phys. Fluids **31**, 359 (1988).